

## Cell-Permeable Bicyclic Peptide Inhibitors against Intracellular Proteins

Wenlong Lian, Bisheng Jiang, Ziqing Qian, and Dehua Pei\*

Department of Chemistry and Biochemistry, The Ohio State University, 484 West 12th Avenue, Columbus, Ohio 43210, United States

### Supporting Information

**ABSTRACT:** Cyclic peptides have great potential as therapeutic agents and research tools but are generally impermeable to the cell membrane. Fusion of cyclic peptides with a cyclic cell-penetrating peptide produces bicyclic peptides that are cell-permeable and retain the ability to recognize specific intracellular targets. Application of this strategy to protein tyrosine phosphatase 1B and a peptidyl-prolyl cis–trans isomerase (Pin1) isomerase resulted in potent, selective, proteolytically stable, and biologically active inhibitors against the enzymes.

Cyclic peptides (and depsipeptides) exhibit a wide range of biological activities.<sup>1</sup> Several innovative methodologies have recently been developed to synthesize cyclic peptides, either individually<sup>2</sup> or combinatorially,<sup>3</sup> and screen them for biological activity. A particularly exciting application of cyclic peptides is the inhibition of protein–protein interactions (PPIs),<sup>4,5</sup> which remain challenging targets for conventional small molecules. However, a major limitation of cyclic peptides is that they are generally impermeable to the cell membrane, precluding any application against intracellular targets, which include most of the therapeutically relevant PPIs. Although the formation of intramolecular hydrogen bonds<sup>6</sup> or N<sup>α</sup>-methylation of the peptide backbone<sup>7</sup> can improve the membrane permeability of certain cyclic peptides, alternative strategies to increase the cell permeability of cyclic peptides are clearly needed.

Protein-tyrosine phosphatase 1B (PTP1B) is a prototypical member of the PTP superfamily and plays numerous roles during eukaryotic cell signaling. Because of its roles in negative regulation of insulin and leptin receptor signaling, PTP1B is a valid target for treatment of type II diabetes and obesity.<sup>8</sup> A large number of PTP1B inhibitors have been reported,<sup>9</sup> but none of them have succeeded in the clinic. Designing PTP inhibitors is challenging because most of the phosphotyrosine (pY) isosteres such as difluorophosphonomethyl phenylalanine (F<sub>2</sub>Pmp)<sup>10</sup> are impermeable to the cell membrane. Additionally, because all PTPs share a similar active site, achieving selectivity for a single PTP has been difficult. In this work, we report a potentially general approach to the design of cell-permeable cyclic peptidyl inhibitors against intracellular proteins such as PTP1B.

We recently discovered cyclo(FΦRRRRQ) (cFΦR<sub>4</sub>, where Φ is L-naphthylalanine) as a novel class of cell-penetrating peptides (CPPs).<sup>11</sup> Unlike previous CPPs, which are typically

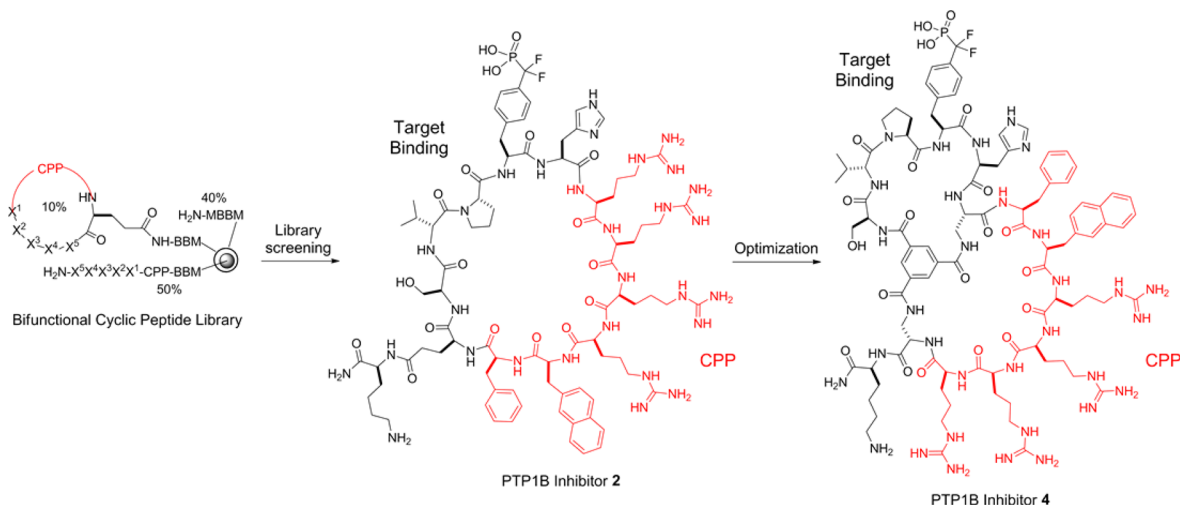
linear peptides that are entrapped in the endosome, cFΦR<sub>4</sub> efficiently escapes from the endosome into the cytoplasm. Short peptide cargos (1–7 amino acids) can be delivered into mammalian cells by incorporating them into the cFΦR<sub>4</sub> ring. Encouraged by this finding, we explored the possibility of developing bifunctional cyclic peptides containing both cell-penetrating and target-binding sequences as cell-permeable inhibitors against intracellular proteins. To generate specific inhibitors against PTP1B, we synthesized a one-bead two-compound library on spatially segregated ChemMatrix resin,<sup>12</sup> in which each bead displayed a bifunctional cyclic peptide on its surface and contained the corresponding linear peptide in its interior as an encoding tag [Scheme 1 and Figure S1 in the Supporting Information (SI)]. The bifunctional cyclic peptides all featured the CPP motif FΦR<sub>4</sub> (or its inverse sequence RRRRΦF) on one side and a random pentapeptide sequence (X<sup>1</sup>X<sup>2</sup>X<sup>3</sup>X<sup>4</sup>X<sup>5</sup>) on the other side, where X<sup>2</sup> represents a 9:1 (mol/mol) mixture of Tyr and F<sub>2</sub>Pmp while X<sup>1</sup> and X<sup>3</sup>–X<sup>5</sup> are any of the 24 amino acids that included 10 proteinogenic L-amino acids (Ala, Asp, Gln, Gly, His, Ile, Pro, Ser, Tyr, Trp), five unnatural α-L-amino acids [F<sub>2</sub>Pmp, L-4-fluorophenylalanine (Fpa), L-norleucine (Nle), L-phenylglycine (Phg), L-pipecolic acid (Pip)], and nine α-D-amino acids [D-Ala, D-Asn, D-Glu, D-Leu, D-β-naphthylalanine (D-Nal), D-Phe, D-Pro, D-Thr, D-Val]. The library has a theoretical diversity of 6.6 × 10<sup>5</sup>. The use of the 9:1 Tyr/F<sub>2</sub>Pmp ratio at the X<sup>2</sup> position, together with a 5-fold reduction of the surface peptide loading, reduced the amount of F<sub>2</sub>Pmp-containing peptides at the bead surface by 50-fold, increasing the stringency of library screening.<sup>13</sup> Screening 100 mg of the library (~300 000 beads/compounds) against Texas red-labeled PTP1B resulted in 65 positive beads, which were individually sequenced by partial Edman degradation–mass spectrometry (PED-MS)<sup>14</sup> to give 42 complete sequences (Table S1 in the SI).

Three representative hit sequences, D-Thr-D-Asn-D-Val-F<sub>2</sub>Pmp-D-Ala-Arg-Arg-Arg-Arg-Nal-Phe-Gln (inhibitor 1), Ser-D-Val-Pro-F<sub>2</sub>Pmp-His-Arg-Arg-Arg-Arg-Nal-Phe-Gln (inhibitor 2), and Ile-Pro-Phg-F<sub>2</sub>Pmp-Nle-Arg-Arg-Arg-Arg-Nal-Phe-Gln (inhibitor 3), were resynthesized and purified by HPLC. All three peptides are competitive PTP1B inhibitors, with peptide 2 being the most potent (IC<sub>50</sub> = 31 ± 3 nM) (Table S2 and Figure S2). Unfortunately, inhibitor 2 showed no significant activity in cellular assays. Confocal microscopy analysis of human cells treated with fluorescein isothiocyanate (FITC)-

Received: April 14, 2014

Published: June 27, 2014

## Scheme 1. Evolution of a Cell-Permeable PTP1B Inhibitor



labeled inhibitor **2** indicated poor cellular uptake of the peptide (Figure 1a). Although disappointing, this result was not entirely

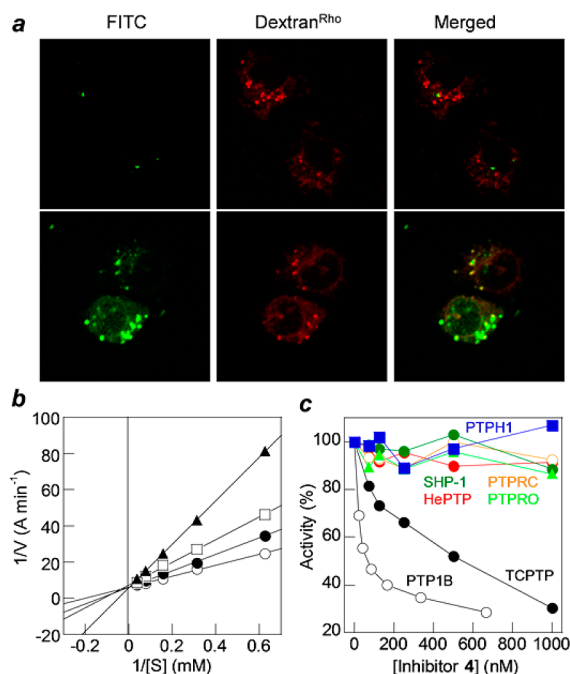


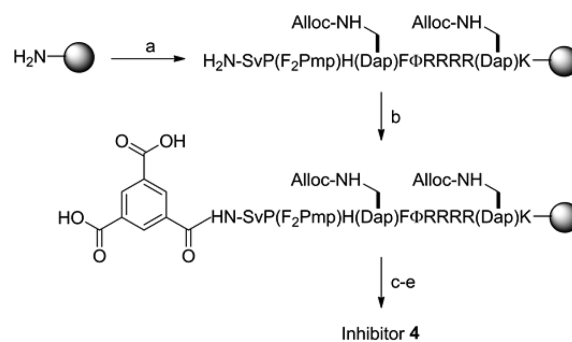
**Figure 1.** (a) Live-cell confocal microscopy images (same Z section) of A549 lung cancer cells after treatment for 2 h with 5  $\mu$ M FITC-labeled inhibitor **2** (top panel) or **4** (bottom panel) and the endocytosis marker dextran<sup>Rho</sup> (1.0 mg/mL). (b) Lineweaver–Burk plot showing competitive inhibition of PTP1B by inhibitor **4** at concentrations of 0 ( $\circ$ ), 28 ( $\bullet$ ), 56 ( $\square$ ), and 112 nM ( $\blacktriangle$ ). (c) Sensitivity of various PTPs to inhibitor **4** (the y axis values are pNPP hydrolysis rates for the PTPs relative to that in the absence of inhibitor). The data shown in (b) and (c) are representative data sets.

unexpected. Our previous study showed that as the size of the cargo inserted into the cF $\Phi$ R<sub>4</sub> ring increased, the cellular uptake efficiency of the cyclic peptides decreased dramatically.<sup>11</sup> We reasoned that larger rings are more conformationally flexible and may bind less tightly to the cell-surface receptors (e.g., membrane phospholipids) during endocytosis. The negatively charged F<sub>2</sub>Pmp may also interact intra-

molecularly with the F $\Phi$ R<sub>4</sub> motif and interfere with its CPP function.

To improve the cell permeability of inhibitor **2**, we explored a bicyclic system in which the CPP motif is placed in one ring whereas the target-binding sequence constitutes the other ring (Scheme 1). The bicyclic system keeps the CPP ring to a minimal size, which according to the previously observed trend<sup>11</sup> should result in more efficient cellular uptake. The bicyclic system should be able to accommodate cargos of any size because incorporation of the latter does not change the size of the CPP ring and therefore should not affect the delivery efficiency of the cyclic CPP. The use of a rigid scaffold (e.g., trimesic acid) may also help keep the CPP and cargo motifs away from each other and minimize any mutual interference. The smaller rings of a bicyclic peptide compared with its monocyclic counterpart should result in greater structural rigidity and improved metabolic stability.

To convert the monocyclic PTP1B inhibitor **2** into a bicyclic peptide, we replaced the Gln residue (used for attachment to the solid support and peptide cyclization) with (*S*)-2,3-diaminopropionic acid (Dap) and inserted a second Dap residue at the junction of the CPP and PTP1B-binding sequences (C-terminal to His) (Scheme 1). Synthesis of the bicycle was accomplished by the formation of three amide bonds between a trimesic acid and the N-terminal amine and the side chains of the two Dap residues (Scheme 2).<sup>5</sup> Briefly,

Scheme 2. Solid-Phase Synthesis of Inhibitor 4<sup>a</sup>

<sup>a</sup>Reagents: (a) standard Fmoc chemistry; (b) trimesic acid, HBTU; (c) Pd(PPh<sub>3</sub>)<sub>4</sub>, *N*-methylaniline; (d) PyBOP; (e) TFA.

the linear peptide was synthesized on Rink amide resin using standard Fmoc chemistry and  $N^{\beta}$ -allocarbonyl (Alloc)-protected Dap. After removal of the N-terminal Fmoc group, the exposed amine was acylated with trimesic acid. Removal of the Alloc groups with Pd(PPh<sub>3</sub>)<sub>4</sub> followed by treatment with PyBOP afforded the desired bicyclic structure. To facilitate labeling with fluorescent probes, a lysine was added to the C-terminus. The bicyclic peptide (peptide 4) was deprotected using trifluoroacetic acid (TFA) and purified to homogeneity by HPLC.

Bicyclic peptide 4 acts as a competitive inhibitor of PTP1B with a  $K_i$  value of  $37 \pm 4$  nM (Figure 1b). It is highly selective for PTP1B. When assayed against PTP1B and TCPTP using *p*-nitrophenyl phosphate (pNPP) as substrate ( $500 \mu\text{M}$ ), inhibitor 4 had  $\text{IC}_{50}$  values of  $30 \pm 4$  and  $500 \pm 250$  nM, respectively (Figure 1c and Table S3). It exhibited minimal inhibition of any of the other PTPs tested ( $\leq 10\%$  inhibition of HePTP, SHP-1, PTPRC, PTPH1, or PTPRO at  $1 \mu\text{M}$  inhibitor concentration). Gratifyingly, inhibitor 4 has greatly improved cell permeability over peptide 2, as detected by live-cell confocal microscopy of A549 cells treated with FITC-labeled inhibitor 4 (Figure 1a). The treated cells showed diffuse fluorescence throughout the cytoplasm and nucleus as well as fluorescence puncta, indicating that a fraction of the inhibitors reached the cytoplasm and nucleus while the rest was likely entrapped in the endosomes. Incubation of inhibitor 4 in human serum for 24 h at  $37^\circ\text{C}$  resulted in  $\sim 10\%$  degradation, whereas 91% of inhibitor 2 was degraded under the same conditions (Figure S3). Overall, inhibitor 4 compares favorably with the small-molecule PTP1B inhibitors reported to date<sup>9</sup> with respect to potency, selectivity over the highly similar TCPTP (17-fold), and cell permeability (Table S4).

Inhibitor 4 was next tested for its ability to perturb PTP1B function during cell signaling. Treatment of A549 cells with inhibitor 4 ( $0\text{--}5 \mu\text{M}$ ) resulted in a dramatic and dose-dependent increase in the pY levels of a large number of proteins, consistent with the broad substrate specificity of PTP1B<sup>15</sup> (Figure 2a). Analysis of the same samples by Coomassie blue staining showed similar amounts of proteins in all of the samples (Figure 2b), indicating that the increased pY levels reflected increased phosphorylation (or decreased PTP reaction) instead of changes in the total protein levels. Remarkably, the increase in tyrosine phosphorylation was already apparent at 8 nM inhibitor 4. Interestingly, further increases in the inhibitor concentration beyond  $1 \mu\text{M}$  reversed the effect on tyrosine phosphorylation, an observation that was also made previously by Zhang and co-workers with a different PTP1B inhibitor.<sup>16</sup> To obtain further evidence that intracellular PTP1B was inhibited by peptide 4, we monitored the pY level of insulin receptor (IR), a well-established PTP1B substrate *in vivo*,<sup>8</sup> by immunoblotting with specific antibodies against the pY<sup>1162</sup>/pY<sup>1163</sup> site. Again, treatment with inhibitor 4 caused a dose-dependent increase in IR phosphorylation up to  $1 \mu\text{M}$  inhibitor, and the effect leveled off at higher concentrations (Figure 2c,d). Taken together, our data indicate that bicyclic inhibitor 4 efficiently entered mammalian cells and inhibited PTP1B *in vivo*. The decreased phosphorylation at higher inhibitor concentrations may have been caused by nonspecific inhibition of other PTPs (which may in turn down regulate protein tyrosine kinases). It may also reflect the pleiotropic roles played by PTP1B, which can both negatively and positively regulate the activities of different protein kinases.<sup>17</sup>

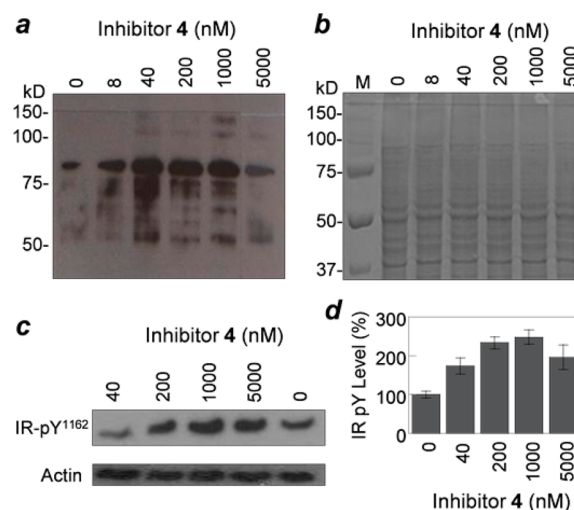
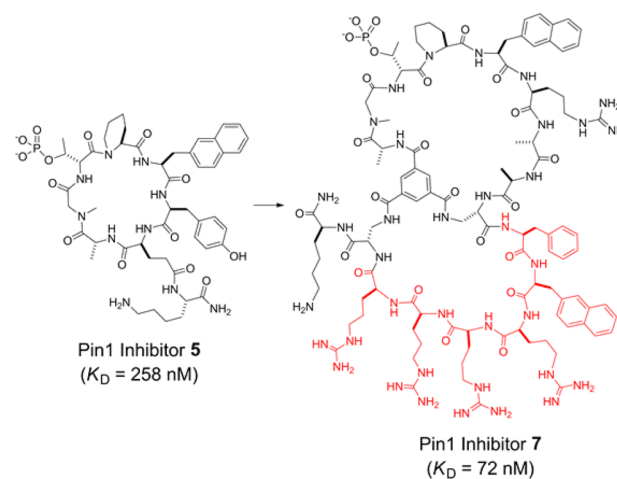


**Figure 2.** Inhibition of PTP1B *in vivo*. (a) Anti-pY immunoblot of global pY protein levels in A549 cells after treatment with  $0\text{--}5 \mu\text{M}$  inhibitor 4 for 2 h. (b) SDS-PAGE analysis (Coomassie blue staining) of the same samples from (a) showing uniform protein loading in all lanes. (c) Effect of inhibitor 4 on insulin receptor phosphorylation at Tyr<sup>1162</sup> and Tyr<sup>1163</sup> sites. HepG2 cells were treated with the indicated concentrations of inhibitor 4 for 2 h, stimulated with insulin ( $100 \text{ nM}$ ) for 5 min, and analyzed by SDS-PAGE and immunoblotting with anti-IRpY<sup>1162</sup>/pY<sup>1163</sup> antibody. (d) Quantitation of IR pY levels from (c) (data shown are means  $\pm$  SD from five independent experiments).

To test the generality of the bicyclic approach, we applied it to the design of cell-permeable inhibitors against peptidyl-prolyl cis–trans isomerase (Pin1), a potential target for treatment of a variety of human diseases, including cancer,<sup>18</sup> for which potent, selective, and biologically active inhibitors are still lacking.<sup>19</sup> Thus, we fused cF $\Phi$ R<sub>4</sub> with the previously reported monocyclic peptide 5, which is a potent inhibitor against Pin1 *in vitro* ( $K_D = 258 \pm 66$  nM) but membrane-impermeable<sup>20</sup> (Scheme 3). In

### Scheme 3. Conversion of Impermeable Pin1 Inhibitor 5 into Cell-Permeable Bicyclic Inhibitor 7



addition, we replaced the L-Tyr at the pThr + 3 position with Arg to improve the aqueous solubility. The resulting bicyclic peptide 6 bound Pin1 with  $K_D = 130 \pm 44$  nM (Table S5 and Figure S4). Insertion of D-Ala at the pThr + 5 position to increase the separation between the Pin1-binding and cell-penetrating motifs improved the inhibitor potency by  $\sim 2$ -fold

( $K_D = 72 \pm 21$  nM for inhibitor 7). Inhibitor 7 competed with FITC-labeled inhibitor 5 for binding to Pin1 (Figure S5), indicating that they both bind to the Pin1 active site. Substitution of D-Thr for D-pThr of inhibitor 7 reduced its potency by ~10-fold ( $K_D = 620 \pm 120$  nM for inhibitor 8; Table S5), whereas further replacement of the pipecolyl residue with D-Ala abolished the Pin1 inhibitory activity (peptide 9). As expected, bicyclic inhibitors 7–9 are cell-permeable (Figure S6). Treatment of HeLa cells with inhibitor 7 resulted in dose-dependent inhibition of cell growth (45% inhibition after treatment for 3 days at 20  $\mu$ M inhibitor 7), whereas the impermeable inhibitor 5 and inactive peptide 9 had no effect (Figure S7). Peptide 8 also inhibited cell growth, but to a lesser extent than inhibitor 7. Finally, treatment of HeLa cells with inhibitor 7 dramatically increased the cellular levels of promyelocytic leukemia protein (PML), an established Pin1 substrate destabilized by Pin1 activity (Figure S8).<sup>21</sup>

In conclusion, we have developed a potentially general approach for the design of cell-permeable bicyclic peptides against intracellular targets. Our preliminary studies show that replacement of the PTP1B-binding motif with other peptide sequences having different physicochemical properties also resulted in their efficient delivery into cultured mammalian cells.<sup>22</sup> The availability of a general intracellular delivery method should greatly expand the utility of cyclic peptides in drug discovery and biomedical research.

## ■ ASSOCIATED CONTENT

### ● Supporting Information

Experimental details and additional data. This material is available free of charge via the Internet at <http://pubs.acs.org>.

## ■ AUTHOR INFORMATION

### Corresponding Author

pei.3@osu.edu

### Notes

The authors declare no competing financial interest.

## ■ ACKNOWLEDGMENTS

This work was supported by NIH (GM062820 and CA132855).

## ■ REFERENCES

- (1) Pomilio, A. B.; Battista, M. E.; Vitale, A. A. *Curr. Org. Chem.* **2006**, *10*, 2075.
- (2) For examples, see: (a) Meutermans, W. D. F.; Golding, S. W.; Bourne, G. T.; Miranda, L. P.; Dooley, M. J.; Alewood, P. F.; Smythe, M. L. *J. Am. Chem. Soc.* **1999**, *121*, 9790. (b) Schafmeister, C. E.; Po, J.; Verdine, G. L. *J. Am. Chem. Soc.* **2000**, *122*, 5891. (c) Sun, Y.; Lu, G.; Tam, J. P. *Org. Lett.* **2001**, *3*, 1681. (d) Kohli, R. M.; Walsh, C. T.; Burkart, M. D. *Nature* **2002**, *418*, 658. (e) Qin, C.; Bu, X.; Zhong, X.; Ng, N. L. J.; Guo, Z. *J. Comb. Chem.* **2004**, *6*, 398. (f) Turner, R. A.; Oliver, A. G.; Lokey, R. S. *Org. Lett.* **2007**, *9*, 5011. (g) Hili, R.; Rai, V.; Yudin, A. K. *J. Am. Chem. Soc.* **2010**, *132*, 2889. (h) Lee, J.; McIntosh, J.; Hathaway, B. J.; Schmidt, E. W. *J. Am. Chem. Soc.* **2009**, *131*, 2122. (i) Frost, J. R.; Vitali, F.; Jacob, N. T.; Brown, M. D.; Fasan, R. *ChemBioChem* **2013**, *14*, 147.
- (3) For examples, see: (a) Eichler, J.; Lucka, A. W.; Pinilla, C.; Houghten, R. A. *Mol. Diversity* **1996**, *1*, 233. (b) Giebel, L. B.; Cass, R. T.; Milligan, D. L.; Young, D. C.; Arze, R.; Johnson, C. R. *Biochemistry* **1995**, *34*, 15430. (c) Scott, C. P.; Abel-Santos, E.; Wall, M.; Wahnnon, D. C.; Benkovic, S. J. *Proc. Natl. Acad. Sci. U.S.A.* **1999**, *96*, 13638. (d) Millward, S. W.; Takahashi, T. T.; Roberts, R. W. *J. Am. Chem. Soc.* **2005**, *127*, 14142. (e) Sako, Y.; Morimoto, J.; Murakami, H.; Suga, H.

*J. Am. Chem. Soc.* **2008**, *130*, 7232. (f) Li, S.; Marthandan, N.; Bowerman, D.; Garner, H. R.; Kodadek, T. *Chem. Commun.* **2005**, 581. (g) Joo, S. H.; Xiao, Q.; Ling, Y.; Gopishetty, B.; Pei, D. *J. Am. Chem. Soc.* **2006**, *128*, 13000. (h) Heinis, C.; Rutherford, T.; Freund, S.; Winter, G. *Nat. Chem. Biol.* **2009**, *5*, 502. (i) Tse, B. N.; Snyder, T. M.; Shen, Y.; Liu, D. R. *J. Am. Chem. Soc.* **2008**, *130*, 15611.

- (4) For examples, see: (a) Leduc, A.-M.; Trent, J. O.; Wittliff, J. L.; Bramlett, K. S.; Briggs, S. L.; Chirgadze, N. Y.; Wang, Y.; Burris, T. P.; Spatola, A. F. *Proc. Natl. Acad. Sci. U.S.A.* **2003**, *100*, 11273. (b) Millward, S. W.; Fiacco, S.; Austin, R. J.; Roberts, R. W. *ACS Chem. Biol.* **2007**, *2*, 625. (c) Tavassoli, A.; Lu, Q.; Gam, J.; Pan, H.; Benkovic, S. J.; Cohen, S. N. *ACS Chem. Biol.* **2008**, *3*, 757. (d) Wu, X.; Upadhyaya, P.; Villalona-Calero, M. A.; Briesewitz, R.; Pei, D. *Med. Chem. Commun.* **2013**, *4*, 378. (e) Birts, C. N.; Nijjar, S. K.; Mardle, C. A.; Hoakwie, F.; Duriez, P. J.; Blaydes, J. P.; Tavassoli, A. *Chem. Sci.* **2013**, *4*, 3046. (f) Kawakami, T.; Ishizawa, T.; Fujino, T.; Reid, P. C.; Suga, H.; Murakami, H. *ACS Chem. Biol.* **2013**, *8*, 1205.

- (5) Lian, W.; Upadhyaya, P.; Rhodes, C. A.; Liu, Y.; Pei, D. *J. Am. Chem. Soc.* **2013**, *135*, 11990.

- (6) Rezaei, T.; Bock, J. E.; Zhou, M. V.; Kalyanaraman, C.; Lokey, R. S.; Jacobson, M. P. *J. Am. Chem. Soc.* **2006**, *128*, 14073.

- (7) (a) Chatterjee, J.; Gilon, C.; Hoffman, A.; Kessler, H. *Acc. Chem. Res.* **2008**, *41*, 1331. (b) White, T. R.; Renzelman, C. M.; Rand, A. C.; Rezaei, T.; McEwen, C. M.; Gelev, V. M.; Turner, R. A.; Linington, R. G.; Leung, S. S. F.; Kalgutkar, A. S.; Bauman, J. N.; Zhang, Y. Z.; Liras, S.; Price, D. A.; Mathiowetz, A. M.; Jacobson, M. P.; Lokey, R. S. *Nat. Chem. Biol.* **2011**, *7*, 810.

- (8) (a) Elchelby, M.; Payette, P.; Michaliszyn, E.; Cromlish, W.; Collins, S.; Loy, A. L.; Normandin, D.; Cheng, A.; Himms-Hagen, J.; Chan, C. C.; Ramachandran, C.; Gresser, M. J.; Tremblay, M. L.; Kennedy, B. P. *Science* **1999**, *283*, 1544. (b) Zabolotny, J. M.; Bence-Hanulec, K. K.; Stricker-Krongrad, A.; Haj, F.; Wang, Y.; Minokoshi, Y.; Kim, Y. B.; Elmquist, J. K.; Tartaglia, L. A.; Kahn, B. B.; Neel, B. G. *Dev. Cell* **2002**, *2*, 489.

- (9) He, R.; Zeng, L.-F.; He, Y.; Zhang, Z.-Y. In *New Therapeutic Strategies for Type 2 Diabetes: Small Molecule Approaches*; Jones, R. M., Ed.; RSC Publishing: Cambridge, U.K., 2012; pp 142 ff.

- (10) Burke, T. R., Jr.; Kole, H. K.; Roller, P. P. *Biochem. Biophys. Res. Commun.* **1994**, *204*, 129.

- (11) Qian, Z.; Liu, T.; Liu, Y.-Y.; Briesewitz, R.; Barrios, A. M.; Jhiang, S. M.; Pei, D. *ACS Chem. Biol.* **2013**, *8*, 423.

- (12) Liu, R.; Marik, J.; Lam, K. S. *J. Am. Chem. Soc.* **2002**, *124*, 7678.

- (13) Chen, X.; Tan, P. H.; Zhang, Y.; Pei, D. *J. Comb. Chem.* **2009**, *11*, 604.

- (14) Thakkar, A.; Wavreille, A.-S.; Pei, D. *Anal. Chem.* **2006**, *78*, 5935.

- (15) Ren, L.; Chen, X.; Luechapanichkul, R.; Selner, N. G.; Meyer, T. M.; Wavreille, A.-S.; Chan, R.; Iorio, C.; Zhou, X.; Neel, B. G.; Pei, D. *Biochemistry* **2011**, *50*, 2339.

- (16) Xie, L.; Lee, S.-Y.; Andersen, J. N.; Waters, S.; Shen, K.; Guo, X.-L.; Moller, N. P. H.; Olefsky, J. M.; Lawrence, D. S.; Zhang, Z.-Y. *Biochemistry* **2003**, *42*, 12792.

- (17) Lessard, L.; Stuibler, M.; Tremblay, M. L. *Biochim. Biophys. Acta* **2010**, *1804*, 613.

- (18) Lu, K. P.; Zhou, X. Z. *Nat. Rev. Mol. Cell Biol.* **2007**, *8*, 904.

- (19) More, J. D.; Potter, A. *Bioorg. Med. Chem. Lett.* **2013**, *23*, 4283.

- (20) Liu, T.; Liu, Y.; Kao, H.-Y.; Pei, D. *J. Med. Chem.* **2010**, *53*, 2494.

- (21) Reineke, E. L.; Lam, M.; Liu, O.; Liu, Y.; Stanya, K. J.; Chang, K. S.; Means, A. R.; Kao, H. Y. *Mol. Cell. Biol.* **2008**, *28*, 997.

- (22) Qian, Z.; LaRochelle, J. R.; Jiang, B.; Lian, W.; Hard, R. L.; Selner, N. G.; Luechapanichkul, R.; Barrios, A. M.; Pei, D. *Biochemistry* **2014**, *53*, 4034–4046.